POLLUTION DISPERSION PREDICTION FOR THE MUST WIND TUNNEL EXPERIMENT WITH ANISOTROPIC ALGEBRAIC MODELS FOR TURBULENT SCALAR FLUXES

R. Izarra-Garcia, J. Franke, W. Frank

Department of Fluid- and Thermodynamics, University of Siegen, Siegen, Germany

Abstract: The numerical prediction of pollution dispersion in urban environments by means of solution of the statistically steady Reynolds Averaged Navier Stokes (RANS) equations is known to be strongly dependent on the turbulence models. In the case of pollution dispersion turbulence models do not only have to be used for the Reynolds stresses but also for the turbulent scalar fluxes. While the influence of several turbulence models for the Reynolds stresses on the dispersion in urban environments has been examined already several times, the turbulent scalar fluxes were exclusively modelled by the simple gradient diffusion assumption. In the present work therefore the influence of more advanced, anisotropic algebraic models for the turbulent scalar fluxes on the dispersion in the MUST wind tunnel experiment is examined. To that end, three anisotropic algebraic flux models were implemented in the commercial software FLUENT 6.3. All these models together with the simple gradient diffusion model (with two turbulent Schmidt numbers) are performed and compared using statistical performance measures to assess their predictive capability.

Key words: *Turbulent scalar fluxes, anisotropic modelling, RANS, CFD, MUST, atmospheric dispersion, model improvement.*

1. INTRODUCTION

In recent times, computational fluid dynamics (CFD) has become a practical tool for the prediction of pollution concentrations in urban areas. Many works can be found in the literature reporting CFD applications to model flow and dispersion for one of building or groups of buildings. The statistically steady Reynolds Averaged Navier–Stokes equation (RANS) method appears to be the most preferable procedures to model dispersion in realistic urban areas due to the relatively low computational costs. Some published works of comparisons between RANS simulations and wind tunnel data show reasonably good agreement. However, the accuracy of results is known to depend on many factors. Besides the most common numerical errors in CFD modelling, e.g. the right computational domain size, adequate grid resolution, numerical boundary conditions, spatial discretisation schemes and any other needed numerical approximation, the turbulence model for the Reynolds stresses plays an important role for the solution of the Navier-Stokes transport equations (Izarra-Garcia et al. 2007). Like the turbulence models for the Reynolds stresses the turbulence models for the scalar fluxes are expected to have an influence on the prediction of concentrations in urban areas.

The general objective of this work is therefore the assessment of advanced anisotropic algebraic models for the turbulent scalar fluxes. These models were created for the application in heat transfer problems with the temperature as passive scalar. Here these models are used for the simulation of passive scalar dispersion within the MUST wind tunnel case used by the COST 732 action *Quality Assurance and Improvement of Micro-Scale Meteorological Models* (URL 1) to analyse possible improvements in urban scale pollution dispersion predictions.

2. MUST EXPERIMENT

The Mock Urban Setting Test (MUST) was a scaled urban dispersion experiment conducted for the Defense Threat Reduction Agency (DTRA) at the U.S. Army Dugway Proving Ground (DPG) Horizontal Grid test site in cooperation with many other institutions. Its objective was to acquire meteorological and dispersion data sets at near full-scale for the development and validation of urban toxic hazard assessment models. MUST was also designed to overcome the scaling and measurement limitations of laboratory experiments and characterization difficulties presented by real urban settings. The experiment consisted of an array of 12 by 10 shipping containers (12.2 m long, 2.4 m wide, and 2.5 m high). The gaps between blocks were spaced to produce a flow regime connecting the wake interference and isolated flow. The array was sufficiently large to create its own internal roughness sub-layer, but sufficiently small to be adequately characterized using available instrumentation (e.g., Yee and Biltoft, 2004).

The same case has been examined by Bezpalcová, K. (2007) in the wind tunnel. She did measurements of the flow fields and concentrations for several approach flow wind direction. The MUST field geometry (without simplifications) was used at scale 1:75. These wind tunnel measurement results are better suited for the evaluation of RANS simulations due to their statistically steady nature. In addition they are reproducible with known uncertainties.

3. NUMERICAL MODEL

Model description

Fluent 6.3 is a general propose computational fluid dynamics software, able to model fluid flow and heat transfer for compressible/incompressible, subsonic/supersonic/hypersonic, laminar/turbulent flows with various options, like chemical reactions, multiphase flows and a solution-based mesh adaption. It solves the governing conservation equations of fluid dynamics with a finite-volume formulation on an unstructured, non orthogonal, curvilinear coordinate grid system. The pressure/velocity field coupling used in this work was the SIMPLE algorithm. The 2nd

order upwind spatial discretization scheme has been used for all convective fluxes. The stopping criteria of the scaled residuals for all variables were always fixed to be below $1 \cdot 10^{-7}$. See FLUENT (2006) for a detailed description of these settings.

Mathematical Model

To perform the numerical simulation of pollution dispersion in a turbulent flow the Navier-Stokes transport equations must be solved together with an additional transport equation for the pollutant's concentration. For the scope of this work the solution is limited to statistically steady flow conditions using the RANS equations.

$$\frac{\partial}{\partial x_j}\left(\rho\overline{u}_i\overline{u}_j + \overline{\tau}_{ij}\right) = -\frac{\partial \overline{p}}{\partial x_i} - \frac{\partial}{\partial x_j}\left(\rho\overline{u_i'u_j'}\right) \tag{1}$$

Using the RANS approach all of the unsteadiness is regarded as part of the turbulence. The Reynolds stresses (term in the right hand side parenthesis) has been modelled using the Realizable k-ε (RKE) and the Launder-Reece-Rodi (LRRIP) Reynolds stress turbulence models. Additionally, a differential equation is solved for the transport of pollutants (ϕ).

$$\frac{\partial}{\partial x_j}\left(\rho\overline{u}_j\overline{\phi}\right) - \frac{\partial}{\partial x_j}\left(\Gamma_\phi \frac{\partial \overline{\phi}}{\partial x_j}\right) = -\frac{\partial}{\partial x_j}\left(\rho\overline{u_j'\phi'}\right) \tag{2}$$

Again in Equation (2), the turbulent scalar flux term (term in the right hand side parenthesis) needs to be modelled. This was done through the implementation of different scalar flux turbulence models into Fluent. The implemented models are the Generalized Gradient Diffusion Hypothesis (GGDH) model from Daly and Harlow (1970), the model from Abe and Suga (2001) (ABE-SUGA) and the model from Abe (2005) (ABE). These models are described in further detail in the following section. In addition the already available standard isotropic Simple Eddy Diffusivity (SED) model was used with two different turbulent Schmidt numbers, Sc_t=0.7 (SED1) and Sc_t=0.9 (SED2).

Algebric scalar flux models

For the general case of a compressible reacting flow with buoyancy effects, the scalar fluxes follow the functional relationship

$$\overline{u_i'\theta'} = F\left(\overline{u_i'u_j'}, S_{i,j}, W_{i,j}, \overline{\phi}_{,j}, \rho, \varepsilon, \phi, g_i, \overline{\phi^2}, \frac{\partial P}{\partial x_j}, \frac{\partial \rho}{\partial x_j}, Ma\right) \tag{3}$$

where Ma is the Mach number and S_{ij} and W_{ij} are the mean rate of strain and mean vorticity tensors, respectively. In case of incompressible flow, a passive scalar, and no gravitational effects, the functional relationship can be written in a general mathematical representation as (Younis et al. 2005)

$$\begin{aligned} -\overline{u_i'\theta'} = {} & \alpha_1\overline{\phi}_{,i} + \alpha_2\overline{u_i'u_j'}\overline{\phi}_{,j} + \alpha_3 S_{ij}\overline{\phi}_{,j} + \alpha_4\overline{u_i'u_k'}\,\overline{u_k'u_j'}\overline{\phi}_{,j} + \alpha_5 S_{ik}S_{kj}\overline{\phi}_{,j} + \\ & + \alpha_6 W_{ij}\overline{\phi}_{,j} + \alpha_7 W_{ik}W_{kj}\overline{\phi}_{,j} + \alpha_8\left(S_{ik}W_{kj} + S_{jk}W_{ki}\right)\overline{\phi}_{,j} + \\ & + \alpha_9\left(\overline{u_i'u_k'}S_{kj} + \overline{u_j'u_k'}S_{ki}\right)\overline{\phi}_{,j} + \alpha_{10}\left(\overline{u_i'u_k'}W_{kj} + \overline{u_j'u_k'}W_{ki}\right)\overline{\phi}_{,j} \end{aligned} \tag{4}$$

where α_i are the model coefficients which in this work are only functions of the turbulent kinetic energy k and its dissipation ε.

All previously cited models are contained in equation (4), using different expressions for the coefficients α_i, with most of them being equal to zero. The SED model uses only $\alpha_1 = \mu_t \cdot Sc_t^{-1}$, the GGDH model only $\alpha_2 = 0.3\tau$ and the ABE-SUGA model only $\alpha_4 = 0{,}45\tau k^{-1}$. The ABE model has two non zero coefficients, $\alpha_2 = 0.22\tau$ and $\alpha_4 = 0.45\tau k^{-1}$. In the above τ is the turbulent time scale defined as $\tau = max[k\,\varepsilon^{-1},\ 6(\mu_{lam}\,\varepsilon^{-1})^{1/2}]$.

All these models do not take wall effects into account except through the definition of τ. To assess the influence of the inclusion of wall effects the damping function proposed by Rokni (1998) was used for the GGDH model, leading to two versions of this model. GGDH2 with wall damping effects and GGDH1 without wall damping effects.

Computational Domain, boundary Conditions and grids

Two computational domains with four grids were used for the simulations. One computational domain is shown in Figure 1a). It was obtained from the computational domain used for the so called 0 degree approach flow case by rotating it around the centre. Therefore the approach flow direction is called –45 degree. Within this domain three systematically refined, block structured grids were created, using only hexahedral cells. These grids will be referred to as *Fine*, *Middle* and *Coarse* in the following. The grids consist of 751,194 cells, 1,552,792 cells and 3,208,752 cells.

The other domain, shown in Figure 1b) was generated by rotating the obstacles inside the wind tunnel geometry. This domain will be referred to as *Std.* Here only one hexahedral grid is used which has the same resolution as the *Middle* grid between the obstacles. Also the vertical resolution is identical.

As boundary conditions for the approach flow a logarithmic profile was used for the velocity component in x-direction, with the same roughness as measured in the wind tunnel. The other two velocity components were set to

zero. The components of the approaching Reynolds stresses were approximated by constant values approximating the measurements above container height. The turbulent kinetic energy k was calculated from the normal Reynolds stresses. The turbulent dissipation rate ε at the inlet was calculated from k under the assumption of local equilibrium (Richards and Hoxey, 1993). These profiles were also used to fix the values at the top boundary at the corresponding height.

As outflow boundary condition a constant pressure was prescribed. The floor was partly treated as rough, like in the wind tunnel. The obstacle walls were treated as smooth walls. Smooth walls were also used as lateral wind tunnel walls for domain *Std*.
Finally, for the concentration the following boundary conditions were used. A value of zero at the inflow boundaries and vanishing normal gradient at all other boundaries. The source was implemented as volumetric source term in the cell that contained the centre of the experimental ground source location.

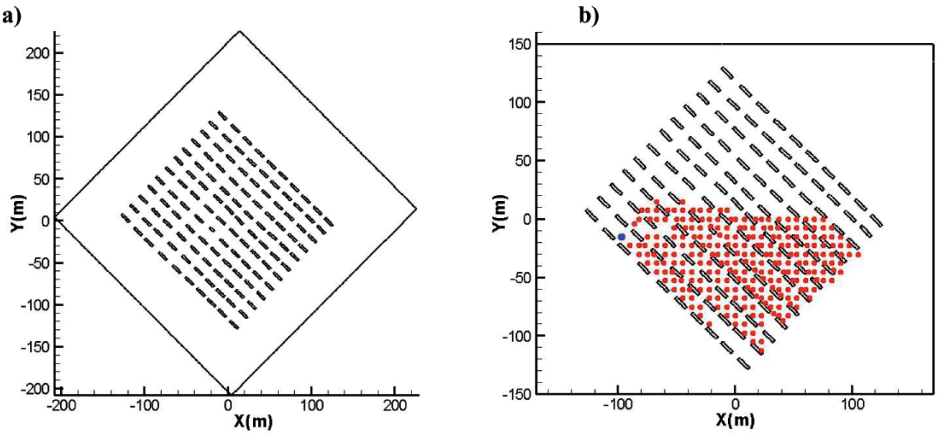

Figure 1. Computational domains for the simulations. a) Rotated domain of the 0 degree approach flow case. b) Wind tunnel domain, also showing source and concentration measurement positions. Wind blows from the left.

4. MODEL EVALUATION

Metrics and hit rate

The concentration data from the wind-tunnel measurements and simulation are normalised as $C^* = C \cdot U_{ref} \cdot H^2 \cdot Q_s^{-1}$, where U_{ref} is the x-velocity at the reference point (x,y,z)=(-144,-2.25,7.29)m, H is the height of the containers and Q_s is the volumetric flow rate of the scalar at the source. Both the flow field and the concentration predictions were evaluated with the aid of the following metrics: factor of two FAC2, fractional bias FB, normalised mean square error NMSE, geometric mean MG and geometric variance VG. They are defined as:

$$FAC\,2 = \text{fraction of data with } 0.5 \le \frac{C_p^*}{C_o^*} \le 2 \tag{5}$$

$$FB = \frac{\overline{C_o^*} - \overline{C_p^*}}{0.5\left(\overline{C_o^*} + \overline{C_p^*}\right)} \tag{6}$$

$$NMSE = \frac{\overline{\left(C_o^* - C_p^*\right)^2}}{\overline{C_o^*} \cdot \overline{C_p^*}} \tag{7}$$

$$MG = \exp\left(\overline{\ln C_o^*} - \overline{\ln C_p^*}\right) \tag{8}$$

$$VG = \exp\left[\overline{\left(\ln C_o^* - \ln C_p^*\right)^2}\right] \tag{9}$$

where the indices "O" and "P" are for the observed and predicted data, respectively. The bar means the average over the entire dataset. The experimental uncertainty of 0.003 for concentrations has been used as threshold, e.g. for the observed and predicted values max(0.003,C*) is used. Chang and Hanna (2004) also give acceptance criteria for these metrics. These limits are FAC2 > 0.5, |FB| < 0.3, NMSE < 4, 0.7 < MG < 1.3 and VG < 1.6. The hit rate is taken from the VDI (2005), defined as:

$$q = \frac{1}{N}\sum_{n=1}^{N} i_n \qquad \text{and} \qquad i_n = \begin{cases} 1 & \text{if } \left|\left(O_n - P_n\right)/O_n\right| \le D \text{ or } \left|O_n - P_n\right| \le W \\ 0 & \text{otherwise} \end{cases} \tag{10}$$

where N is the number of measurement positions, D (=0.25) is the allowed relative difference and W (=0.003 for concentrations) is the allowed absolute difference. The recommended hit rate acceptance criterion is $q \geq 0.66$. The metrics and hit rate have been calculated for the 256 single valued measurement positions of the concentrations.

5. RESULTS

The metrics for the concentrations are listed in Table 1. The analysis of the flow field is not the main interest of this work; therefore it is not shown in detail. However, the same evaluation procedure was followed for the flow and a very good agreement was found for both, the LRRIP and RKE model.

Table 1. Metrics for the six models for the five simulations.

		FB	MG	NMSE	VG	FAC2	q
1) Std-LRRIP	SED1	-0.12	0.95	2.07	1.09	0.97	0.84
	SED2	-0.24	0.90	3.13	1.13	0.95	0.69
	GGDH1	-0.22	0.89	2.51	1.18	0.94	0.82
	GGDH2	-0.22	0.89	2.50	1.17	0.94	0.82
	ABE-SUGA	-0.31	0.87	4.92	1.49	0.81	0.67
	ABE	-0.06	1.02	4.01	1.24	0.93	0.78
2) Fine-LRRIP	SED1	-0.33	0.83	4.34	1.53	0.80	0.52
	SED2	-0.37	0.82	5.17	1.81	0.69	0.49
	GGDH1	-0.34	0.83	7.16	2.01	0.72	0.49
	GGDH2	-0.34	0.83	7.16	2.00	0.73	0.49
	ABE-SUGA	-0.35	0.86	13.04	2.94	0.68	0.49
	ABE	-0.25	0.88	10.99	1.71	0.78	0.68
3) Middle-LRRIP	SED1	-0.33	0.82	3.49	1.35	0.86	0.59
	SED2	-0.35	0.83	4.14	1.51	0.79	0.52
	GGDH1	-0.29	0.84	5.52	1.69	0.76	0.51
	GGDH2	-0.29	0.84	5.51	1.69	0.76	0.51
	ABE-SUGA	-0.25	0.89	10.32	2.32	0.71	0.53
	ABE	-0.23	0.87	8.28	1.55	0.82	0.73
4) Coarse-LRRIP	SED1	-0.36	0.83	4.79	1.53	0.81	0.54
	SED2	-0.40	0.82	5.67	1.80	0.70	0.47
	GGDH1	-0.37	0.82	8.07	2.07	0.71	0.45
	GGDH2	-0.37	0.82	8.05	2.06	0.71	0.45
	ABE-SUGA	-0.36	0.84	12.51	3.23	0.67	0.45
	ABE	-0.29	0.86	10.61	1.75	0.78	0.68
5) Std-RKE	SED1	-0.05	0.98	0.67	1.12	0.96	0.76
	SED2	-0.19	0.89	1.26	1.10	0.98	0.70
	GGDH1	0.17	1.13	0.86	1.27	0.82	0.70
	GGDH2	0.17	1.13	0.86	1.27	0.82	0.70
	ABE-SUGA	0.24	1.20	1.27	1.35	0.79	0.68
	ABE	0.51	1.41	2.85	1.77	0.67	0.59

Richardson extrapolation as used by Franke, J. and W. Frank (2008) was tried to quantify the numerical error due to spatial discretisation with the three systematically refined meshes. However, most of the measurement positions showed divergent behaviour making Richardson extrapolation impossible. Therefore only the grid sensitivity of the results can be assessed by the results presented in Table 1. From there it can be seen that most of the metrics show oscillating behaviour. This indicates that the results are likely to change with further grid refinement, which is definitely required to allow for the quantification of the numerical error. The present grids are not all in the asymptotic range, which is necessary for Richardson extrapolation.

For the concentrations most of the results are inside of the acceptance criteria recommended by Chang and Hanna (2004). An exception is the NMSE which is more often larger than 4. It is very interesting how in the rather complex MUST case the most simple and well known model SED1 (with Sc_t=0.7) performed best for most of the evaluation parameters considered here. However, when using the LRRIP Reynolds stress turbulence model the anisotropic models from ABE and GGDH are nearly as good as the SED1 model. The differences between the GGDH1 and GGDH2 model are negligible, indicating that the distance of the wall for the first computational nodes is so large that wall damping does not have any effect. An easy general ranking can be seen from the FAC2 and the hit rate records. Both are very robust measures for the agreement between measurement and numerical prediction. Interesting are the considerably good results that have been obtained for the recently published ABE model. While the results are

sometimes even better than the ones for the SED1 model, the ABE model is not of common use yet. The worst predictions for the LRRIP runs are given by the ABE-SUGA model. For these runs a consistent overprediction of concentrations can be observed, represented by the negative values of FB and MG lower than 1. The locations of this overprediction are mostly close to the source for all models.

Another result from Table 1 is that the usage of the computational domain which replicates the experimental set up (Std-LRRIP) yields the best results for the concentrations. This can be very well seen from NMSE. While it is always larger than 4 for the domain LRRIP-Middle, except for SED1, only the simulations using the ABE and ABE-SUGA models have these high values for the domain Std-LRRIP. As both domains have the same grid resolution between the containers these differences are most likely due to the different boundary conditions.

When using the RKE turbulence model for the Reynolds stresses the concentration results are changed considerably. While the results for SED1 and SED2 do not change much, the metrics of the anisotropic models show substantial differences in the flow field. As can be seen from the now always positive FBs (and the MGs > 1) the models now yield an underprediction of concentrations on the average. Comparing the anisotropic models it is seen that now the ABE model has the worst results. The most likely reason for the worse performance of the anisotropic models is the worse prediction of Reynolds stresses with the k-ε based RKE model as the Reynolds stresses are a very important parameter for all the anisotropic scalar flux models presented here.

Finally, it can be stated that the SED2 model with Sc_t = 0.9, which is the value often used in heat transfer applications, does lead to worse results than the SED1 model with the standard value of Sc_t = 0.7. Other authors even recommend lower values than 0.7 (Di Sabatino et al., 2007; Tominaga and Stathopoulos, 2007).

6. CONCLUSIONS

The prediction capability of different scalar flux model has been evaluated for the MUST wind tunnel test case through the use of statistical metrics. The simple SED model has been proven in many previous works to fail in simple heat transfer applications. However, for the dispersion in the MUST case it gives satisfactory results for most of the evaluation parameters using Sc_t=0.7. This is not the case for a different Sc_t. It was also found that the modelling of turbulent scalar fluxes by anisotropic models is highly related to the prediction accuracy of the Reynolds stresses. Therefore the anisotropic scalar flux models are expected to be most accurate when using Reynolds stress turbulence models for the flow field. From the GGDH model variations it could be observed that the big size of the cells close to walls, which is common for micro-scale simulations, supersedes the necessity of wall damping functions in urban scale pollution dispersion applications.

REFERENCES

Abe, K., 2006: Performance of Reynolds-averaged turbulence and scalar-flux models in complex turbulence with flow impingement. *Progress in Computational Fluid Dynamics*, **6**, 79-88.

Abe, K. and K. Suga, 2001: Towards the development of Reynolds-averaged algebraic turbulent scalar-flux model. *International Journal of Heat and Fluid Flow*, **22**, 19-29.

Bezpalcová, K., 2007: Physical Modelling of Flow and Dispersion in an Urban Canopy, PhD thesis, Faculty of Mathematics and Physics, Charles University, Prague, 193pp.

Chang, J.C. and S.R. Hanna, 2004: Air quality performance evaluation. *Met. and Atm. Physics*, **87**, 167-196.

Daly, B. and F. Harlow, 1970: Transport Equations in Turbulence. *The Physics of Fluids*, **13**, 2634-2649.

Di Sabatino, S., R. Buccolieri, B. Pulvirenti and R.E. Britter, 2007: Flow and Pollutant Dispersion in Street Canyons using FLUENT and ADMS-Urban. *Environ. Model. Assess.*, **13**, 369-381.

FLUENT, 2006: Fluent V6.3 User's Guide, Fluent Inc., USA, 2501pp.

Franke, J. and W. Frank, 2008: Application of generalised Richardson extrapolation to the computation of the flow across an asymmetric street intersection. *J. of Wind Eng. and Ind. Aerodyn.*, in press. doi:10.1016/j.jweia.2008.02.003

Izarra-Garcia, R., J. Franke and W. Frank, 2007: CFD simulation of pollution dispersion in a 2D Street canyon, Int. Scientific Conference microCAD 2007, Miskolc, March 22-23.

Richards, P. J. and R.P. Hoxey, 1993: Appropriate boundary conditions for computational wind engineering models using the k-ε model. *Journal of Wind Engineering and Industrial Aerodynamics,* **46&47,** 145-153.

Rokni, M., 1998: Numerical Investigation of Turbulent Fluid Flow and Heat Transfer in Complex Ducts, Doctoral thesis, Department of Heat and Power Engineering, Lund Institute of Technology, Sweden.

Tominaga, Y. and T. Stathopoulos, 2007: Turbulent Schmidt numbers for CFD analysis with various types of flowfield. *Atmospheric Environment*, **41**, 8091-8099.

VDI, 2005: Environmental meteorology – Prognostic micro-scale windfield models – Evaluation for flow around buildings and obstacles. VDI guideline 3783, Part 9, Beuth, Berlin, 53 pp.

Yee, E. and C.A. Biltoft, 2004: Concentration Fluctuation Measurements in a Plume Dispersing Through a Regular Array of Obstacles. *Boundary-Layer Meteorology*, **111**, 363-415.

Younis, B., Ch. Speziale and T. Clark, 2005: A rational model for the turbulent scalar fluxes. *Proc. of the Royal Soc. A.*, **461**, 575-594.

URL 1: Official web site of COST 732: http://www.mi.uni-hamburg.de/index.php?id=464